Sizing the Electrical Grid

Omid Ardakanian, S. Keshav, and Catherine Rosenberg
University of Waterloo
Technical Report CS-2011-18

***Abstract*—Transformers and storage batteries in the electrical grid must be provisioned or sized just as routers and buffers must be sized in the Internet. We prove the formal equivalence between these two systems and use this insight to apply teletraffic theory to sizing the electrical grid, obtaining the capacity region corresponding to a given transformer and storage size. To validate our analysis, we conduct a fine-grained measurement study of household electrical load. We compare numerical simulations using traces from this study with results from teletraffic theory. We show not only that teletraffic theory agrees well with numerical simulations but also that it closely matches with the heuristics used in current practice. Moreover, our analysis permits us to develop sizing rules for battery storage electrical grid, advancing the state of the art.**

I. Introduction

JUST as Internet Service Providers size links and routers in the Internet, electric utilities size line and transformer capacities in the electrical grid to be large enough to meet expected peak loads, but not so large as to be too expensive [1]. In both networks, operators use rules of thumb to roughly estimate resource sizing, upgrading capacity piecemeal as dictated by demand growth.

Two trends motivate us to re-examine current design rules for sizing the electrical grid. First, there is expected to be a worldwide surge in grid deployment in the next decade. In the developed world, infrastructure put into place during the rapid postwar growth phase of the 1950's and 1960's is reaching the end of its operational life and must be replaced in the next 10 to 20 years. This is a good time, therefore, to re-examine sizing guidelines.

Second, with the incorporation of renewable energy sources and battery-operated electric vehicles, it is expected that the future grid would have non-trivial amounts of storage [2]. The classical grid has had little storage and provisioning storage is poorly understood. As a result, there is a need to understand how to provision storage in the future grid.

An obvious question is the relevance of these developments to researchers in the computer networking community. The answer to this question is twofold. First, the theory of large deviations, which is the basis of the teletraffic analysis, enables us to study the asymptotic behaviour of a tail probability of the sum of independent random variables. These random variables could represent work brought to a queue in a computer network or the amount of energy brought to a storage battery in the electrical grid. In this paper, we investigate the power of this theory by applying it to the electrical grid and show that the results are consistent with our observations in computer networks. Second, as discussed in [3], both the Internet and the electrical grid are designed to meet fundamental needs by connecting geographically dispersed suppliers with geographically dispersed consumers. Therefore, there are many areas where we can apply the concepts and techniques that are commonly used in the Internet to the electrical grid and *vice versa*. The key insight of this paper is that *mathematical techniques from teletraffic theory can be used to size the electrical grid.* We make three specific contributions:

- We prove a formal equivalence between transformers and storage in the grid and routers and buffers in a network, allowing us to use teletraffic theory to analyse the grid
- We provide design rules for provisioning storage in the grid and study the insights gained from these rules
- We show that sizing decisions made using our design rules compares well with the 'ground truth' sizing obtained by directly measuring loads and, moreover, can lead to gains over existing sizing techniques

The rest of the paper is organized as follows. We present an overview of the electrical grid in Section II. The equivalence between a distribution branch in the grid and a network is shown in Section III. We use this equivalence to obtain grid design rules using teletraffic theory in Section IV. We present a measurement study and discuss how we can use our measurements to validate our analysis in Section V. The results of this work are presented in Section VI. We survey related work in Section VII. We discuss our contributions in more detail in Section VIII and conclude in Section IX.

II. Background

The electrical grid consists of three subsystems: generation, transmission, and distribution [4]. Electrical power generators use energy from sources such as coal, natural gas, or falling water to generate alternating currents. These currents flow into a transmission system that moves electric power to distribution networks. The transmission network, like the Internet core, has a mesh structure to meet reliability requirements of the grid. To minimize resistive losses, it operates at very high voltages of 150-500kV. Power from the transmission network is stepped down using transformers before entering the tree-like distribution network, which delivers power from distribution substations to end customers. This structure is analogous to the delivery of video content from content servers in centralized data centres over the Internet core and access networks to end-systems.

Step-down transformers are necessary for distribution networks to interface with the long-distance transmission system. A transformer's capacity or 'size' is the sustained power that it can deliver, measured in kilo Volt Amperes or kVA. Although this rating can be exceeded on rare occasions, grid design rules require that no transformer exceed its rating for more than short time intervals.

Transformers can be expensive. A small pole-top 167kVA single-phase distribution transformer that serves about 10 homes in North America costs around $3,000 [5]. A typical small utility serving a customer base of 30,000 homes would therefore need to spend $9,000,000 on poletop distribution transformers alone. High-voltage transformers at substations, which serve thousands of customers, can cost up to $1,500,000.

Sizing a transformer is a critical design decision. A utility could potentially save millions of dollars by choosing smaller transformer sizes when replacing ageing equipment. On the other hand, underestimating the size of a transformer might lead to overloading that would shorten its life, and in the worst case, lead to transformer failure and power outage.

Several issues make transformer-sizing non-trivial. First, like MPEG-encoded video, electrical loads (i.e., the power requested by a home as a function of time, measured in Watts) are highly variable, making it unrepresentative to describe them by their mean values alone. On the other hand, sizing a transformer for peak load may be both overly conservative and expensive. Second, transformers are deployed for twenty to fifty years with only periodic maintenance. Because the load may change over this time, accurate load forecasting must be done. Third, the electrical grid has strict reliability criteria, which, if not met, can lead to dangerous overheating of transformers. To deal with these constraints, utilities use a conservative approach to size transformers. This approach typically results in oversized transformers and lightly used, expensive infrastructure. Our work is the first step in coming up with better sizing guidelines that can help utilities to optimize their infrastructural expenditure without reducing system reliability.

The transformer sizing problem is exacerbated by the imminent widespread availability of energy storage, particularly in the form of battery-electric vehicles. By storing energy during non-peak hours and releasing it to meet peak load, which is known as peak shaving, it will be possible to use a smaller transformer in the presence of energy storage. However, the relationship between storage and transformer sizing is currently an open problem. There is, therefore, an urgent need for design rules for distribution systems that incorporate storage.

A. System Description

We study sizing a transformer shared by a set of homes. These transformers, in the North American context, could be either 'poletop' transformers that are shared by 10-25 homes, or larger pad-mounted transformers that are shared by up to several thousand homes [4]. Going beyond current practice, we assume that the poletop or substation may also contain storage to offset peak loads. Our goal is to jointly size the transformer and the storage to make sure that system reliability constraints are met[1].

In choosing transformer size, it is important to ensure system reliability. Reliability is measured by the *loss-of-load probability (LOLP)* [4], which is the probability that the system-wide generation resources fall short of demand. The "one-day-in-ten-years" criterion ($LOLP = 2.74 \times 10^{-4}$) is a benchmark value widely used among utilities in the United States.

This existing definition of reliability has one shortfall: it accounts for generation resources but not storage. The introduction of storage into the grid changes the classical picture of grid reliability because even if the transformer cannot meet the instantaneous aggregated demand, it is possible that the residual demand (i.e., the demand minus the transformer rating) can be met by storage. Therefore, in our work, we say that the reliability criterion is not met when demand cannot be met by a transformer even in the presence of storage because the store is currently empty, so that the demand results in a store underflow. Then, given a transformer rating and a storage size, we use the probability of storage underflow for a particular set of demands as a measure of the loss-of-load probability.

B. Model and Notation

In the rest of the paper, we study a single distribution branch of the electrical grid associated with a transformer with rating C Volt Amperes and a battery or store with capacity B Watt-hours (Figure 1a). These are shared by a set of n homes, indexed by i. Each home places a load of $L_i(t)$ watts on the system at time t. We call the sum of the home loads at any time as the $aggregated$ load at that time. We assume that each home's load can be categorized as belonging to one of N load classes, with n_j homes in the jth load class. We assume conservatively that the generator produces energy at constant rate that exceeds C so that it is not a bottlenecked resource. We also assume the presence of a power conversion system, marked 'PCS', that charges the store whenever the aggregate load is smaller than C and meets demand from the store whenever the aggregate load exceeds C.

III. A Queueing Model for the Grid

To achieve our top level goal of determining sizing rules for storage in the electrical grid, we begin by constructing a queueing system to model a distribution branch in the grid. We proceed in two steps. First, we develop an intuitively appealing equivalence between a branch of the distribution grid and a simple computer network in Section III-A. Then, in Section III-B, we formalize our intuition by showing that an electrical grid with storage can be modelled as a non-traditional $D/G/1/B$ queueing system that can, nevertheless, be analysed as a standard $G/D/1/B$ queue.

A. State Evolution Equivalence

We compare the branch of the electrical grid shown in Figure 1a with a shared buffer of size B bytes accessed by a communication channel of capacity C bits/second shared by a set of sources, indexed by i, and with a transmission rate of $L_i(t)$ bits/second in Figure 1b.

We first consider the evolution of the shared store in the grid. If the sum of demands is less than C, then the store

[1]Note that we do not study systems with electric vehicles in the home, although our analysis can be extended to cover this scenario.

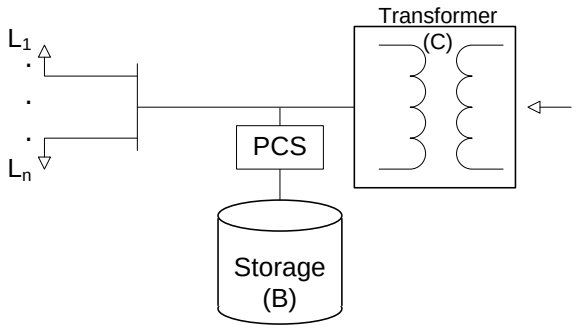

(a) A branch of the electrical grid with n loads L_i where the capacity of the battery is B Watt-hours and the base rating of the transformer is C Volt Amperes. The Power Conversion System (PCS) drains and fill the store depending on load conditions.

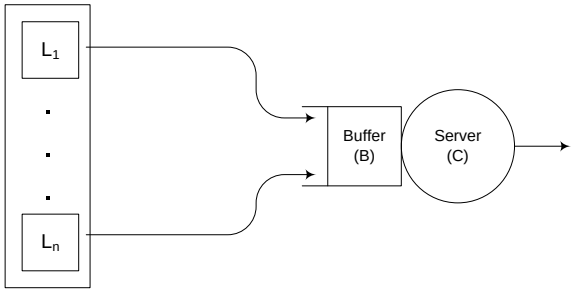

(b) A $G/D/1/B$ fluid queue with n sources L_i. The capacity of the buffer is B bytes and the service rate of the server is C bytes/second.

Fig. 1: The storage system and a small network.

charges at the rate $C - \sum_i L_i(t)$, unless it is full. Denoting the amount of energy in the store (i.e., its *workload*) at time t by $W(t)$, we write this as:

$$dW(t)/dt = \begin{cases} C - \sum_i L_i(t) & \text{if } (W(t) < B), \\ 0 & \text{otherwise} \end{cases}$$

Symmetrically, if the sum of loads exceeds C, then the store can be used to supply energy to the homes, unless the store is empty, in which case the voltage supply received by the homes will drop, which can be viewed as a failure of reliability. We write this as:

$$dW(t)/dt = \begin{cases} C - \sum_i L_i(t) & \text{if } (W(t) > 0), \\ 0 & \text{otherwise} \end{cases}$$

Combining the two, we write

$$dW(t)/dt = \begin{cases} C - \sum_i L_i(t) & \text{if } (0 < W(t) < B), \\ 0 & \text{otherwise} \end{cases} \quad (1)$$

Now, consider the rate at which the network buffer changes over time. Denote the amount of information in the buffer at time t by $\overline{W}(t)$. If the sum of the arrival rates from the sources exceeds C, then the excess arrivals are stored in the buffer if space permits. Therefore, we can write:

$$d\overline{W}(t)/dt = \begin{cases} \sum_i L_i(t) - C & \text{if } (\overline{W}(t) < B), \\ 0 & \text{otherwise} \end{cases}$$

On the other hand, if the sum of arrivals is less than C, then the buffer drains out at the rate $C - \sum_i L_i(t)$ unless it is empty, in which case its drain rate is 0. We write this as

$$d\overline{W}(t)/dt = \begin{cases} \sum_i L_i(t) - C & \text{if } (\overline{W}(t) > 0), \\ 0 & \text{otherwise} \end{cases}$$

Combining the two, we can write:

$$d\overline{W}(t)/dt = \begin{cases} \sum_i L_i(t) - C & \text{if } (0 < \overline{W}(t) < B), \\ 0 & \text{otherwise} \end{cases} \quad (2)$$

Comparing equations 2 and 1, we see that they are symmetrical. This suggests that it should be possible to model the two queueing systems analogously. We formalize this intuition next.

B. Equivalent Queueing Models

Observe that the queueing model corresponding to our electrical storage system is a $D/G/1/B$ fluid queue. This is because electrical power generated at a constant rate C is precisely a fluid arrival bringing work to the system at the deterministic rate C. Moreover, the load from home i can be viewed as a fluid service rate, so that the service rate corresponding to the aggregate load $\sum_{i=1}^{n} L_i(t)$ that drains the buffer can be modelled as a G (general) service-rate process[2] The critical aspect of this queueing system that we want to quantify is its *underflow* probability, i.e., the probability that a service finds the store empty. Unfortunately, standard queueing models do not deal with this question.

However, teletraffic analysis can be used to analyse the standard $G/D/1/B$ queueing system [6]. Based on the intuition from the previous section, our plan of attack is to show that we can model a $D/G/1/B$ system with an equivalent $G/D/1/B$ system, permitting use of teletraffic analysis.

Let the *workload trajectory* of a queue denote a specific instance of the function $W(t)$, i.e., the store size at time t. Let $W(\infty)$ denote the stationary workload process [7]. Our main theoretical result is the Equivalence Theorem:

Equivalence Theorem *Every workload trajectory in the $D/G/1/B$ queuing system corresponds to an equivalent trajectory in the $G/D/1/B$ queuing system such that $\forall t, W(t) + \overline{W}(t) = B$.*

Proof can be found in the Appendix □.

One consequence of the Equivalence Theorem is that the probability of storage underflow in the storage system is precisely the probability of buffer overflow in the network

[2]Note that, if $\lambda = E(\sum_i L_i)$ is the average service rate then typically, for this queueing system, $C > \lambda$, i.e., we have a finite queue with a utilization factor $\rho > 1$.

system (Corollary 1 in the Appendix). The latter probability has been thoroughly investigated in teletraffic theory, to which we turn to next.

IV. Sizing the Grid

This section briefly states standard results from teletraffic theory to compute approximations for the overflow probability in a $G/D/1/B$ system in both bufferless and buffered systems under the assumption that the arrivals are Markovian. We validate our use of teletraffic theory in Section V

We make the technical assumptions that each individual load $L_i(t)$ is stationary and Markovian. Let Y_i be this stationary distribution. Let Y be the stationary distribution of the aggregate load. Without storage, C has to be dimensioned so as to allow for large variations in the aggregate load (i.e., peaks). By introducing finite storage, we will be able to dimension C less conservatively. If $B = \infty$, then there is no overflow and the system is stable as long as $\lambda < C$. Typically, our requirement is that the overflow probability in the original system is less than a desired small value ϵ, which corresponds to LOLP target, typically 2.7×10^{-4}.

A. Bufferless Case

We can write our requirement as:

$$\log P(Y \geq C) \leq -\beta = \log \epsilon \tag{3}$$

Following Kelly [6], we use Chernoff's bound to obtain:

$$\begin{aligned} \log P(Y \geq C) &\leq \log E[e^{sY}] - sC \\ &\leq \inf_s \{\log E[e^{sY}] - sC\} \end{aligned}$$

Where $\log E[e^{sY}]$ is the logarithm of the moment-generating function of Y. Then, the effective bandwidth of a source with the stationary fluid generation rate Y is given by

$$\alpha(s) = \frac{1}{s} \log E[e^{sY}] \tag{4}$$

An improved approximation for the loss probability can be derived using the approach of El Walid *et al* [8]:

$$P(Y \geq C) \sim \frac{e^{s^*(\alpha(s^*)-C)}}{s^*(2\pi\sigma^2(s^*))^{\frac{1}{2}}} \quad as \quad C \to \infty \tag{5}$$

where s^* is a point where $s(\alpha(s) - C)$ attains its infimum, and $\sigma^2(s)$ is defined as follows:

$$\sigma^2(s) = \frac{\partial^2}{\partial s^2}(s\alpha(s))$$

Hence, given the aggregate load Y, C can be computed so that the overflow probability is less than ϵ.

We are also interested in understanding how a mix of loads can impact the sizing of the transformer. Assume that loads belong to N classes where all loads in a class are i.i.d. and loads from different classes are mutually independent. Then, if $\alpha_j(s)$ is the effective bandwidth of a home in class j, the aggregate effective bandwidth is

$$\alpha(s) = \sum_{j=1}^{N} \alpha_j(s)$$

Therefore, if we approximate $\log P(Y \geq C)$ by $\inf_s\{s(\alpha(s) - C)\}$, the capacity region; i.e., the values of C that satisfy (3), will be:

$$Capacity \quad region = \{C | \inf_s \{s(\sum_{i=1}^{N} n_i\alpha_i(s) - C)\} \leq -\beta\} \tag{6}$$

This is an asymptotic formula, i.e., the formula is valid under the assumption that the total number of sources is large and we are interested in the tail of the distribution.

B. Buffered Case

Here, our first goal is to compute the overflow probability in a system given C and B. For this we compute

$$\log p(W(\infty) \geq B) \tag{7}$$

where $W(\infty)$ is the stationary distribution of the workload. Whitt [7] states several different asymptotic forms for the steady state distribution of the workload of stable queues. Of these, we focus on the exponential tail approximation of the workload for large buffers originally studied by ElWalid *et al* [8], *i.e.*,

$$p(W(\infty) \geq B) \sim e^{-nc_1}e^{-c_2B} \quad as \quad B \to \infty \tag{8}$$

where e^{-nc_1} is the loss probability in the bufferless case (see Equation 5). To find the loss probability of the buffered case (i.e., the overflow probability), we only need to compute c_2. It can be shown that $-c_2$ is the dominant eigenvalue of a buffered multiplexing system which determines the tail behaviour of the workload, and for Markovian sources, we can compute it by finding the solution of the following problem [9] [8]:

$$f(z) = \sum_{j=1}^{N} n_j MRE(R_{j_d} - \frac{1}{z}Q_j) - C = 0 \tag{9}$$

Where MRE gives the maximal real eigenvalue of a matrix, n_j is the number of sources in class j, and R_{j_d} and Q_j are the diagonal traffic generation rate matrix and intensity matrix of sources in class j respectively.

Now, we are interested in the capacity region so that

$$\log p(W(\infty) \geq B) \leq -\beta = log\epsilon \tag{10}$$

we have:

$$Capacity \quad region = \{C | \log(\frac{e^{s^*(\alpha(s^*)-C)}}{s^*(2\pi\sigma^2(s^*))^{\frac{1}{2}}}) + zB \leq -\beta\} \tag{11}$$

This is an asymptotic formula, i.e., the formula is valid under the assumption that the number of sources is large, the buffer is large, and we are interested in the tail of the distribution.

To sum up, teletraffic analysis allows us to associate an overflow probability (or LOLP) with a particular choice of B and C as $n \to \infty$ and for a given Markovian aggregate workload $\sum_i L_i(t)$. We view these as our 'design rules' that allow us to size transformer and storage capacities, i.e., a (C, B) tuple, to meet the demands of a given workload with a certain reliability constraint.

V. Validation of Our Approach

Our modelling and analysis of storage systems in the electrical grid allows us to use teletraffic theory to determine transformer and storage sizing rules. Teletraffic theory makes a number of strong assumptions about the nature of the workload. Are the results of teletraffic analysis really applicable to the electrical grid? This section describes our approach to answering this critical question.

Our overall approach is to use real measurements of electrical load to empirically determine the storage and transformer sizes needed to serve them. We then compare the sizes so determined with those determined from teletraffic analysis. We show that the results obtained in these two ways are comparable. An overview of our approach is shown in Figure 2. We explain the details of this approach in the remainder of this section.

A. Obtaining Real Demand Workloads

Our first step is to obtain real measurements of electrical load. In this paper, we focus on residential loads rather than commercial or industrial loads.

Detailed models for residential loads have been presented in the power engineering, environmental studies, and civil engineering literature [10]–[13]. However, these models suffer from two problems. First, the data sets on which these models are based are not publicly available. Second, to the best of our knowledge, existing models group all homes into a single class. Our measurements show significant differences in demand behaviour at different homes. Therefore, it would be better to model each class of home differently, which is the approach that we follow in our analysis. This is also the approach followed by electric utilities.

To obtain our own load data set, we built a testbed to measure aggregate loads at 20 homes. We deployed measurement nodes at 19 houses and one home-based small business covering a range of living area sizes, occupants, appliances, and energy consumption patterns. For the purpose of our small pilot study, we used a convenience sample rather than a stratified random sample. Our methodology generalizes to samples chosen using standard population sampling techniques [14].

Each measurement node consists of a Current Cost Envi device [15] and a netbook. The Envi device measures the power consumption of a house every six seconds and stores it locally in flash memory[3]. A script on the netbook queries the device every six seconds to obtain an XML file that it stores on disk. This is uploaded using a secure SSL connection to a server in our lab once a day. To preserve privacy of the participants in our study, logs files are anonymized before being stored in a secure directory on the file server.

Typical loads from three of four types of houses for one week are shown in Figure 3, with the busy hours marked with vertical lines.

[3]Consequently, the device does not capture load transients that last shorter than this time.

B. Assumptions for Empirical Sizing

We now turn our attention to using our load measurements to sizing transformers and storage in the grid. Suppose we had fine-grained load measurements from all the homes in one neighbourhood for a period of several years. Then, we could simply add these to create the true aggregate load. Given the aggregate load, a trivial numerical simulation suffices to determine the aggregate duration of service disruption corresponding to a particular transformer sizing and a particular storage size. This simulation uses the discretized version of Equation 2 to update the state of the store given a particular demand and transformer size, recording the durations of underflow.

However, it is impractical to measure all the loads from a neighbourhood for several years before making a sizing decision. Moreover, even if such a trace were to be obtained, it would be difficult to determine the degree to which the trace would be representative of other neighbourhoods or of the same neighbourhood two decades hence. Therefore, we have to make the following assumptions even when doing an empirical sizing of transformers and storage:

1) Household energy demands can be categorized into a few distinct classes corresponding to sampling strata, where demands within a class are homogeneous and the classes are mutually exclusive.
2) The homes selected for measurement in our study are a representative random sample of their assigned class.
3) The proportion of homes selected for measurement is representative of the true proportion of homes in each class.

These assumptions are rather strong, but can be removed if homes chosen for measurement were chosen from a stratified random sample, which we would advocate in a real-world application of our design rules. In this case, the aggregate load in Figure 2 would be a reasonably good representative of the true aggregate load.

C. Empirical Sizing

Given the assumptions in Section V-B, we now consider the problem of empirically determining the size of a transformer and storage pair for a residential neighbourhood.

We use the following methodology. First, we sum the load traces of different homes over a period of time to find the aggregate power consumption. A typical aggregate load is shown in Figure 4. Second, we use this aggregate power consumption in a numerical simulation to obtain the aggregate duration of load disruption corresponding to a particular transformer and storage sizing. We note that a similar approach can be used by an electric utility to empirically size storage $without$ needing to use teletraffic analysis. The results from this numerical simulation are presented in Section VI.

D. Teletraffic-based Sizing

As discussed earlier, using teletraffic theory to size transformers and storage has several advantages over an empirical approach. Indeed, applying the theory allows us to readily compute the effect of varying the number of homes, the buffer

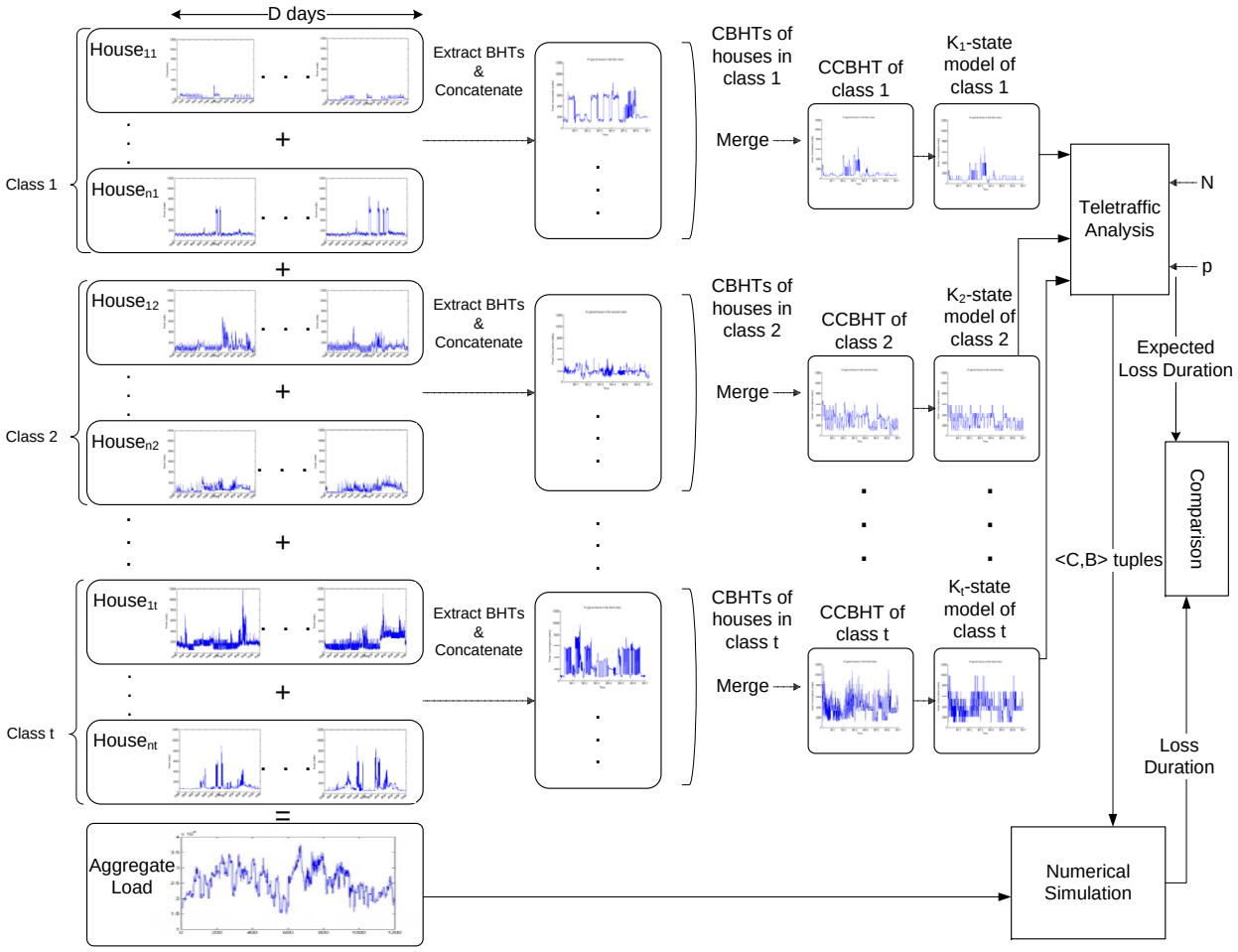

Fig. 2: An overview of our validation methodology.

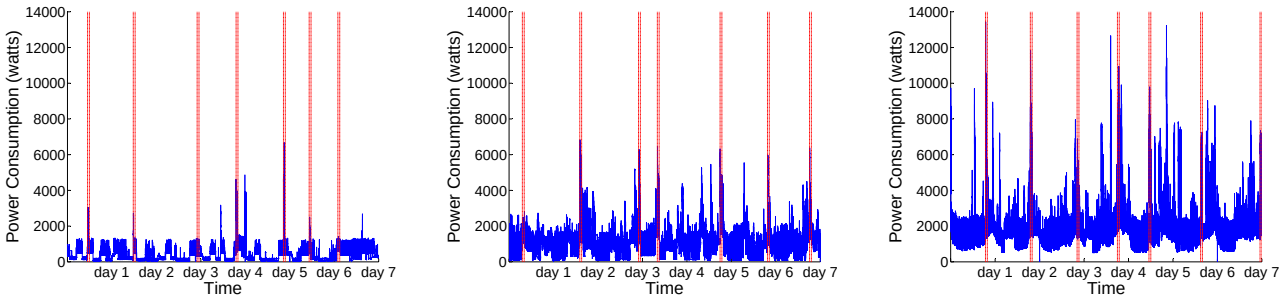

Fig. 3: Load measurements from houses in three classes for one week with busy hours marked by vertical lines.

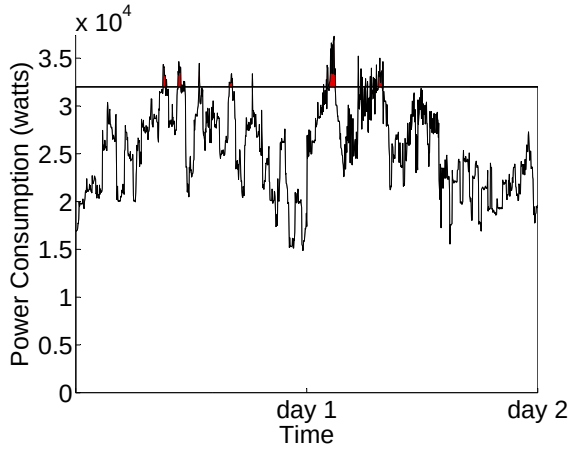

Fig. 4: An example of the aggregate workload over a period of two days. The shaded areas above the horizontal line represent the times when demand is met from the store for a transformer size of 32.4 kiloWatts.

size, or the proportion of the homes in each class without having to recompute or re-measure the aggregate load and run onerous numerical simulations.

To gain these advantages, however, we need to make some additional assumptions about the nature of electrical demands. These are:

4) The electrical demand during the *busy hour* (defined below) at each home is a conservative upper bound on its demand.
5) The cumulative busy hour trace (CBHT) of a home represents the typical busy hour demand of a home.
6) CBHTs from different homes in the same class can be concatenated to represent the aggregate demand from the class. We call the concatenated cumulative busy hour traces the CCBHTs.
7) CCBHTs are independent.
8) CCBHTs are adequately represented by a k-state continuous-time Markov model. This implicitly assumes that busy hour behaviour is stationary and ergodic.
9) Asymptotic limits can be used even for the fairly small number of homes and CCBHTs in our study.

We note that using the busy hour to size the system is the standard approach used in telecommunication systems. This is the one-hour period during which a home uses the most energy (it may or may not include the daily peak power point). It is generally accepted that a sizing that is based on the busy hour alone is more conservative than that using the entire day and therefore provides a sufficient cushion against measurement bias and lack of complete measurement data.

Our methodology for the teletraffic-based sizing is as follows. First, based on Assumption 4, we find the busy hour for each home for each day. This is the one-hour period with the maximum area under the power consumption profile (see Figure 2). Usually, the busy hour happens during the peak hours, i.e., 7am-11am and 5pm-9pm during the winter[4]. We call the load during the busy hour for a home as its 'Busy Hour Trace' or BHT. Second, we concatenate the BHTs of each home for a specific number of days to obtain the cumulative busy hour trace (CBHT) for that period[5]. This represents the typical peak demand of the home according to Assumption 5. Third, based on Assumption 6, we concatenate CBHTs of homes in the same class to get the concatenated CBHT (CCBHT) of that class, which represents its busy hour behavior. Figure 5 shows the typical CCBHT of three of four classes in our measurement study. Fourth, we use Assumption 8 to extract a Markov model for each class. These Markov models are building blocks of the teletraffic sizing algorithm described in Section V-D1.

We jointly validate assumptions 5-9 by comparing the loss duration predicted by teletraffic analysis to those computed by numerical simulation in Section VI. Note that the last three assumptions are technical assumptions needed for teletraffic analysis.

1) Creating a Markov Model for a Class: Home loads are due to the superposition of loads from different electrical appliances [10]. Both the literature and our observations suggest that each appliance can be modeled as an ON-OFF source with exponentially distributed ON and OFF periods. An appliance i consumes P_{ON_i} watts when it is ON, and P_{OFF_i} watts when it is OFF (usually, P_{OFF_i} is zero). Therefore, it is plausible that the power consumption of a class can be modelled as a k-state continuous-time Markov process. However, this still leaves the assignment of power levels to Markov states open.

To address this issue, we use the *k-means* clustering algorithm to cluster the CCBHT for each class into k levels. Using these levels, we construct a modified CCBHT by substituting a measured power consumption value with the value of the center point of the cluster that it belongs to. Since k is an unknown, to determine the appropriate value of k for each class, we run the clustering algorithm with different values of k. Then we use the goodness-of-fit metric introduced in [16] to find the minimum number of states necessary for representing the home load of a class in a period.

2) The Teletraffic-based Sizing Algorithm: Given the set of Markov models, one for each class, using teletraffic theory to compute sizing requires four additional steps. First, we compute the power consumption rate matrix, R, and the intensity matrix, Q, of each class from its modified CCBHT as follows. The rate matrix represents the amount of power consumed by houses in each state. Values of the center points of the clusters (in the clustered CCBHTs) that are found for a given value of k are elements of the power consumption rate matrix, R. The intensity matrix specifies how fast the amount of power consumption is changed. We construct the intensity matrix of the Markov models by finding the average time that it takes to transition from the state i to the state j, which gives us $1/q_{ij}$ (q_{ij}s are elements of the intensity matrix, Q).

Second, from the Q matrix we compute the stationary probability distribution of the continuous-time Markov process. Suppose that π_i is the stationary probability of being in state

[4]All our measurements have been obtained during the winter.

[5]Note that the length of this period is not necessarily equal to the length of load traces used in numerical simulation

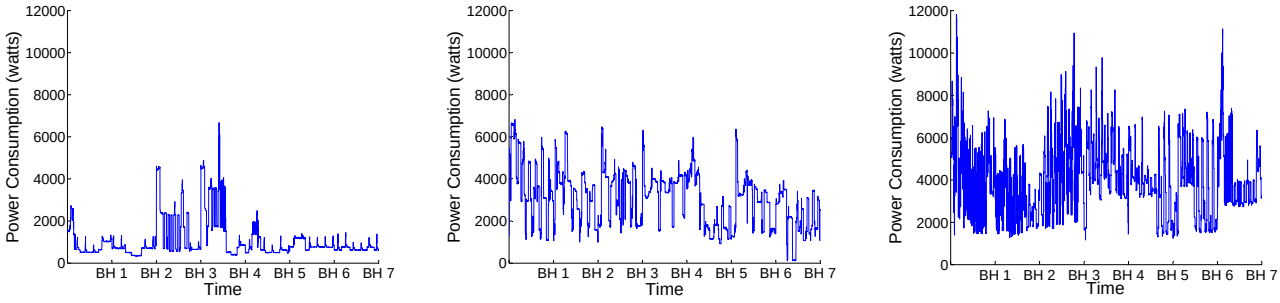

Fig. 5: CCBHTs for three classes for one week.

i, we write the moment generating function of the stationary power consumption of a Markovian source

$$M(s) = \sum_i \pi_i e^{sr_i} \tag{12}$$

where r_i is the power consumption in state i.

Third, using the moment generating function of a Markovian source we can derive a formula for the effective bandwidth (see Equation 4). El Walid $et\ \ al$ prove that the effective bandwidth of a Markovian source is the maximal real eigenvalue of the matrix $R_d - \frac{1}{z}Q$, where $R_d = diag(R)$ [17].

Finally, in the fourth step, we use the approximations in Equations (5) and (8), to find (C, B) tuples such that for a given number of houses from each class, the loss probability is less than a specific value. To allow us to study distribution branches with different numbers of houses than in our study, we assume that the proportion of houses in class i, say ρ_i, is constant and known. Therefore, if we have n houses, the number of houses in class i is $n\rho_i$, which we can then use in our teletraffic-based design rules.

VI. Results

We present our results in four parts. First, we describe the methodology by which we placed home loads into one of four classes. Second, we validate our use of teletraffic theory by comparing the aggregate duration of load outage, for a particular sizing, obtained using numerical simulations and teletraffic analysis. Third, we compare the sizing obtained from our model with those used by a major electricity utility in our geographical area. Finally, we use teletraffic models to study the behaviour of the electrical grid in response to changes in transformer and storage sizing. This allows us to gain insights into the operation of this complex system.

A. Classifying Home Loads

Home electricity loads are highly variable and depend on factors such as the number of occupants, the time of day, the season, mean household income, and the types of appliances commonly in use in the geographical area. Given this variability, choosing a classification for home loads is a challenging task. Fortunately, standard rules based on decades of field experience allow an electric utility to both predict and classify a home load based on a few simple parameters.

Type of Heating	House Size			
	$100m^2$	$200m^2$	$300m^2$	$400m^2$
Baseboard electric heat	3.0	4.0	5.0	6.0
Central electric heat	4.0	5.0	6.0	7.0
Gas/oil heat, no central A/C	1.0	1.5	2.0	2.5
Gas/oil heat, central A/C	1.5	2.5	3.5	4.5
For town or row houses, multiply the unit value by 0.8.				

TABLE I: 'Unit values' assigned to customer homes by a major utility.

Class	Unit value	Number of houses
1	1.2	8
2	2.5	7
3	3.5	3
4	4.5	2

TABLE II: Number of homes in our experiment within each class.

We obtained such a parametrization, specifically used for transformer sizing, from a major utility in our area (Table I). The key sizing parameters are the house size and the nature of the heating and cooling systems, which constitute the major loads in our geographical area. These are used to compute a 'unit value' that represents the load expected from that home.

To minimally impact participant privacy, we asked each participant to tell us their home's unit value computed using this table. We then placed homes with the same unit value in the same class. Table II shows the four classes so obtained. We computed the CCBHTs for the homes in each class as discussed in Section V to carry out teletraffic analysis, and these are shown in Figure 5.

B. Comparing Results from Numerical Simulation and Teletraffic Theory

We used both teletraffic theory and numerical simulations to compare the expected aggregate duration of load disruption for the set of 20 homes in our measurement study keeping the LOLP fixed at 2.74×10^{-4}. Our teletraffic-based sizing results are from the concatenation of the busy hour traces extracted from a week of measurement.

For a particular LOLP, we computed equivalent pairs of (B,

LOLP	(B,C) tuples (Watt-TimeUnits, kVA)	Teletraffic theory (TimeUnits)	Numerical simulation (TimeUnits)
2.74×10^{-4}	(B=0 , C= 107.27)	55.24	0
	(B=10^4 , C= 97.83)	55.24	0
	(B=10^5 , C= 79.27)	55.24	0
	(B=10^6 , C= 70.07)	55.24	0
	(B=10^7 , C= 68.55)	55.24	0
	(B=10^8 , C= 68.36)	55.24	0
	(B=10^9 , C= 68.34)	55.24	0

TABLE III: Loss duration for 14 days of measurements conducted in 20 houses. The time unit is six seconds.

LOLP	(B,C) tuples (Watt-TimeUnits, kVA)	Teletraffic theory (TimeUnits)	Numerical simulation (TimeUnits)
2.74×10^{-4}	(B=0 , C= 636.35)	39.46	0
	(B=10^4 , C= 629.43)	39.46	0
	(B=10^5 , C= 590.72)	39.46	0
	(B=10^6 , C= 551.00)	39.46	0
	(B=10^7 , C= 544.06)	39.46	0
	(B=10^8 , C= 543.19)	39.46	0
	(B=10^9 , C= 543.08)	39.46	0

TABLE IV: Loss duration for 100 days for synthetic data for 100 statistically identical houses. The time unit is one minute.

C) values, as shown in Table III. We chose a wide range of B values and computed the corresponding C values. Note that B values are in Watt-TimeUnits, where one TimeUnit is the granularity of our measurement, i.e., six seconds. Therefore, a B value of 10^4 Watt-TimeUnits, for example, is $10^4/10$ Watt-minutes or 16.7 Watt-hours. Also note that we converted the transformer size obtained from teletraffic analysis from Watt to Volt-Ampere (VA) by dividing it by the *power factor*; we set the power factor to 0.9.

Given a (B, C) pair, we used numerical simulation to compute the actual duration of load disruption. The length of load traces used in the numerical simulation is 14 days. Table III compares the duration of load outage predicted using the two techniques. We see that the predictions from theory closely match simulation results.

To compensate for the limited duration of our trace and to additionally validate our approach, we also synthetically generated the electricity demand for 100 homes for 100 days using a 1-minute-grain simulator developed at the University of Loughborough [10]. This workload generator has been shown to closely approximate real domestic demands. To generate this synthetic trace, we chose all the homes to have four occupants and with a randomly selected mix of appliances. All other values were those set by default including the occupancy pattern. The subsequent modelling and analysis of this data set was identical to that used for our own data set. However, it represents both a homogeneous load population as well as a much longer CCBHT for load modelling. Table IV shows the results of this comparison. We again see that predictions from teletraffic analysis are consistent with ground truth.

To further validate our results, we computed load models from the entire 24-hour trace, rather than just the busy hour both for our data set and the synthetic data set. We compared predictions from this load model with numerical simulations

Total unit value	Transformer size (kVA)
1-3	10
4-9	25
10-24	50
25-36	75
37-50	100
51-88	167

TABLE V: Transformer sizing rules used by a major utility.

over the entire 24-hour trace. Using load traces from our measurement study, we found that for all LOLPs and for all values of B, the predictions were a tight upper bound on the simulation results. However, using the synthetic data set, our predictions were not consistent with results of numerical simulation. We attribute this to the fact that the entire day traces from this data set are highly correlated whereas if we confine our study to a short window of time, like the busy hour, the correlation of load traces decreases drastically. Therefore, we advocate the use of busy hours in the teletraffic-based sizing algorithm. Due to lack of space, we do not present the sizing results obtained using the entire 24-hour trace.

C. Comparing Our Sizing with Industry Practice

The transformer sizing rules used by a major utility in our geographical area are shown in Table V. We now compare the sizing obtained by using our analysis and these rules.

The total unit value of the 20 homes in our study was 46.6. Thus, for the industry standard LOLP of 2.74×10^{-4} the transformer size is 100 kVA. From Table III, we predict that for the same LOLP with no storage, the transformer size should be 107.27 kVA. This is in excellent agreement with the heuristics used by the utility. This indicates that a careful load modelling based on measurements matches heuristics developed over decades of field experience, validating our analysis.

Note that had the sum of unit values been even slightly larger (greater than 50), the heuristic would have advocated a size of 167 kVA, which would have been 56% greater than strictly necessary to meet the LOLP. Even greater savings can be achieved by adding storage. For example, our analysis indicates that, for the same set of homes, by adding 10^6 Watt-time units, or 1.67 kWh of storage, keeping LOLP at 2.74×10^{-4}, it is possible to reduce the transformer size from 107.27 kVA to 70.07 kVA, a reduction of 35%. This does not mean that installing this amount of storage is cost-efficient. It has been discussed in [18] that most of the applications of energy storage are cost-prohibitive with current technologies and prices. However, energy storage brings a mix of benefits to both end-user customers and the grid. Therefore, if we quantify all its benefits, we might conclude that it is economical; this is clearly beyond the scope of this paper.

D. The Effect of Storage on the Electrical Grid

We now use teletraffic analysis to study the insights embodied by our design rules, that is, the inter-relationship between transformer size C, the storage size B, the number of homes n and the loss probability p.

We first study the effect of storage size and loss probability on transformer size for 20 homes (Figure 6). Here, we find that

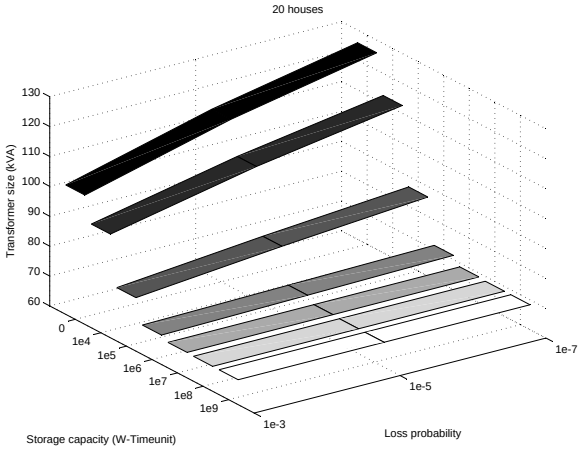

Fig. 6: The effect of storage size and loss probability on transformer capacity for 20 homes.

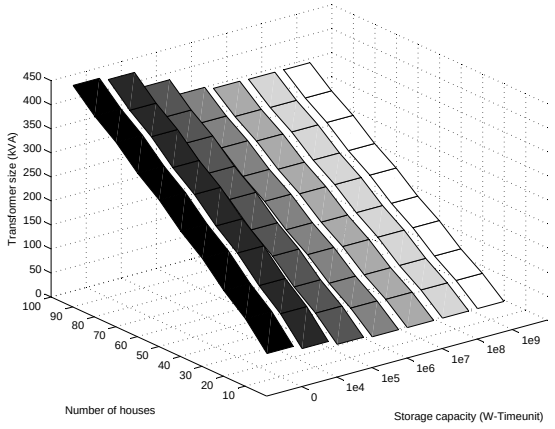

Fig. 7: The effect of number of homes and storage size on transformer capacity for a fixed loss probability of 2.74×10^{-4}(10-100 houses).

the addition of storage has a perceptible impact on transformer sizing. For 20 homes, as we go from no storage to 1.67 kWh of storage, the required transformer size, for a fixed loss probability, goes down by about 40%. Interestingly, we find that the transformer size increases fairly sharply as the loss probability measure becomes more stringent. However, by adding storage, we can gain the same level of reliability without increasing the transformer size. Moreover, we observe than the effect of adding storage on transformer capacity for 20 homes diminishes for storage sizes greater than 1.67 kWh.

We next keep the loss probability fixed and vary both the number of homes n and the storage size (Figures 7, and 8). For both small and large n the required transformer size increases linearly with the number of houses. This is a straightforward consequence of representing a house by its 'effective bandwidth.' We also see that for small values of n, as the storage size increases, the transformer size required decreases significantly, demonstrating that the addition of storage allows us to reduce transformer capacity. However, for large values of n, storage appears to have only moderate effect, a well-known phenomenon in the Internet [19].

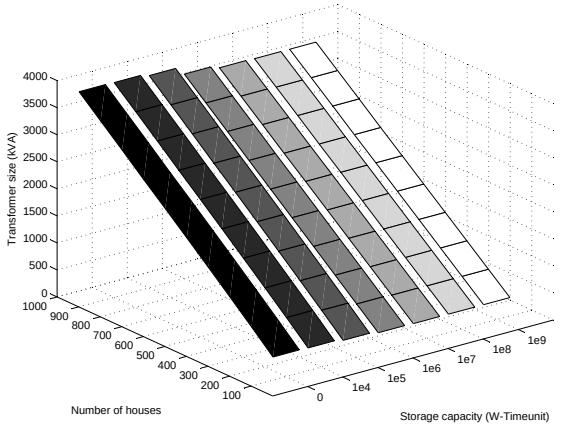

Fig. 8: The effect of number of homes and storage size on transformer capacity for a fixed loss probability of 2.74×10^{-4}(100-1000 houses).

VII. Related Work

Transformer sizing in the electrical grid is usually studied in the context of overall distribution system planning. The standard approach to solve the problem is to use linear optimization [1], [20]. However, this approach necessarily models loads using only their peak values, ignoring temporal variations. These models also do not take storage into account.

Storage can be used both to even out variations in demand, as we study, as well as variations in supply, especially in the context of variable-rate generation by wind turbines and photovoltaic cells: see Divya and Ostergaard [21] and Deshmukh et al [22] for further details and a survey of current work in this area. To the best of our knowledge, most prior work on the effect of storage in the power grid has been on the supply side, and has not used concepts from teletraffic theory. For example, Lee and Gushee [2] compute the amount of storage needed across the entire United States to smooth out variations in wind energy generation. Similarly, Roy et al have studied the optimal sizing of batteries to even out variations in a single wind turbine [23]. Although they use the same equations to model the evolution of battery state as we do, their analysis is based on numerical simulations or the simplifying assumption that the generation process follows a Weibull distribution.

The use of storage to deal with variations on the demand side was proposed by Lachs as early as 1995 [24]. However, the lines of work closest to ours are by Ponnambalam et al and Kempton et al. Ponnambalam, et al use a novel moment-based method to study the battery storage process [25]. This approach is complex and relies on stochastic programming rather than teletraffic models. Kempton et al have studied the use of electrical vehicles for supplying energy to the grid, which they term "Vehicle-to-Grid" [26]. Their analysis focuses more on the details of vehicle usage and charging rates than

the battery storage process.

VIII. Discussion and Future Work

Our work has made several simplifying assumptions. First, we have already noted that teletraffic design rules are meant to be used in the asymptotic regimes for the number of houses, storage capacity, and transformer capacity. Although these asymptotes are arguably achieved for storage capacity (10^7 Watt-TimeUnits) and transformer size (10^4 VA) in our measurement study, they are certainly not achieved for the number of houses. Therefore, we caution the use of these rules for small distribution networks: they are far more applicable deeper in the distribution tree. Unfortunately, lacking data from a sufficiently large number of houses, we were forced to apply our techniques to the small-n regime.

Second, network buffers can be filled and drained with no perceptible degradation. In contrast, the lifetime of a battery may depend on the depth of discharge, especially for Lithium-ion cells [27]. This is due to the buildup of electrolytic deposits in the battery, and degradation of the anode [28]. In addition, the lifetime also may depend on the temperature of use and the exact charging voltage. These effects are difficult to quantify, making the use of teletraffic analysis only one piece of a complex puzzle. Incorporation of battery dynamics into the system model without overly complicating the analysis is an exciting area for future work.

Third, although our work was motivated by the need to re-examine design rules for time-varying generation from renewable energy sources, this paper does not deal with this issue. We believe, however, that $G/G/1/B$ teletraffic analysis can be used to study time-varying Markovian generation systems.

Despite these limitations, we believe that the use of teletraffic analysis to model and size electrical grids represents an exciting area of multi-disciplinary work. We hope to use our approach in the future to answer questions such as:

- If home-owners also own electric vehicles so that there is storage at each home, is shared storage in the distribution system necessary or cost effective?
- If a home generates electricity according to a stochastic process that models wind or photovoltaic generation, how does this affect the sizing and operations of the in-home and shared store?

IX. Conclusion

We revisit the rules for sizing elements of the electrical grid motivated by the replacement of ageing infrastructure and the anticipated increase in storage deployment. Instead of modelling loads by their peak values and using linear optimization, the standard approach in power systems, our work presents a new approach to define design rules for distribution systems. The basis of our work is the Equivalence Theorem, which states that a battery in the electrical grid can be modelled as a buffer in a network. This permits us to apply teletraffic analysis to size the electrical grid. We validate our approach by using our own measurement data as well as synthetic data. Our results show that our approach is in good agreement both with numerical simulations and industry practice.

References

[1] W. El-Khattam, Y. Hegazy, and M. Salama, "An integrated distributed generation optimization model for distribution system planning," *IEEE Trans. Power Systems*, vol. 20, no. 2, pp. 1158–1165, 2005.

[2] B. Lee and D. Gushee, "Massive electricity storage," *AIChE White Paper, AIChE Government Relations Committee*, 2008.

[3] S. Keshav and C. Rosenberg, "How internet concepts and technologies can help green and smarten the electrical grid," *SIGCOMM Comput. Commun. Rev.*, vol. 41, pp. 109–114, 2011.

[4] A. Meier, *Electric Power Systems: A Conceptual Introduction*. Wiley-IEEE Press, 2006.

[5] "General electric transformer pricing," http://www.geindustrial.com/catalog/buylog/20_BL.pdf, January 2011.

[6] F. Kelly, *Notes on Effective Bandwidth*. Oxford University Press, 1996, pp. 141–168.

[7] W. Whitt, *Stochastic-Process Limits - An Introduction to Stochastic-Process Limits and Their Application to Queues*, ser. Springer Series in Operations Research and Financial Engineering. Springer, 2002.

[8] A. Elwalid, D. Heyman, T. V. Lakshman, D. Mitra, and A. Weiss, "Fundamental bounds and approximations for ATM multiplexers with applications to video teleconferencing," *IEEE JSAC*, vol. 13, no. 6, pp. 1004–1016, 1995.

[9] D. Anick, D. Mitra, and M. M. Sondhi, "Stochastic theory of a data handling system with multiple sources," *Bell System Technical Journal*, vol. 61, pp. 1871–1894, 1982.

[10] I. Richardson, M. Thomson, D. Infield, and C. Clifford, "Domestic electricity use: A high-resolution energy demand model," *Energy and Buildings*, 2010.

[11] M. Armstrong, M. Swinton, H. Ribberink, I. Beausoleil-Morrison, and J. Millette, "Synthetically derived profiles for representing occupant-driven electric loads in Canadian housing," *J. of Building Performance Simulation*, vol. 2, no. 1, pp. 15–30, 2010.

[12] A. Capasso, W. Grattieri, R. Lamedica, and A. Prudenzi, "A bottom-up approach to residential load modeling," *IEEE Trans. Power Systems*, vol. 9, no. 2, pp. 957–964, 2002.

[13] J. Paatero and P. Lund, "A model for generating household electricity load profiles," *International J. of Energy Research*, vol. 30, no. 5, pp. 273–290, 2006.

[14] W. Cochran, *Sampling techniques*. John Wiley & Sons Inc, 1977.

[15] "Current cost," http://www.currentcost.com/, January 2011.

[16] O. Ardakanian, S. Keshav, and C. Rosenberg, "Markovian models for home electricity consumption," in *Proc. ACM SIGCOMM Green Networking Workshop*, 2011.

[17] A. Elwalid and D. Mitra, "Effective bandwidth of general markovian traffic sources and admission control of high speed networks," *IEEE/ACM ToN*, vol. 1, no. 3, pp. 329 –343, Jun. 1993.

[18] W. J. Culver, "High-value energy storage for the grid: A multi-dimensional look," *The Electricity Journal*, vol. 23, no. 10, pp. 59 – 71, 2010.

[19] G. Appenzeller, I. Keslassy, and N. McKeown, "Sizing router buffers," in *Proc. of ACM SIGCOMM*, 2004, pp. 281–292.

[20] K. Aoki, K. Nara, T. Satoh, M. Kitagawa, and K. Yamanaka, "New approximate optimization method for distribution system planning," *IEEE Trans. Power Systems*, vol. 5, no. 1, pp. 126–132, 1990.

[21] K. Divya and J. Østergaard, "Battery energy storage technology for power systems–An overview," *Electric Power Systems Research*, vol. 79, no. 4, pp. 511–520, 2009.

[22] M. Deshmukh and S. Deshmukh, "Modeling of hybrid renewable energy systems," *Renewable and Sustainable Energy Reviews*, vol. 12, no. 1, pp. 235–249, 2008.

[23] A. Roy, S. Kedare, and S. Bandyopadhyay, "Application of design space methodology for optimum sizing of wind-battery systems," *Applied Energy*, vol. 86, no. 12, pp. 2690–2703, 2009.

[24] W. Lachs and D. Sutanto, "Uncertainty in electricity supply controlled by energy storage," in *Proc. Energy Management and Power Delivery*, vol. 1. IEEE, 1995, pp. 302–307.

[25] K. Ponnambalam, Y. Saad, M. Mahootchi, and A. Heemink, "Comparison of methods for battery capacity design in renewable energy systems for constant demand and uncertain supply," in *7th Intl. Conf. on the European Energy Market*. IEEE, 2010, pp. 1–5.

[26] W. Kempton and J. Tomic, "Vehicle-to-grid power fundamentals: Calculating capacity and net revenue," *J. Power Sources*, vol. 144, no. 1, pp. 268–279, 2005.

[27] S. Peterson, J. Apt, and J. Whitacre, "Lithium-ion battery cell degradation resulting from realistic vehicle and vehicle-to-grid utilization," *J. Power Sources*, 2009.

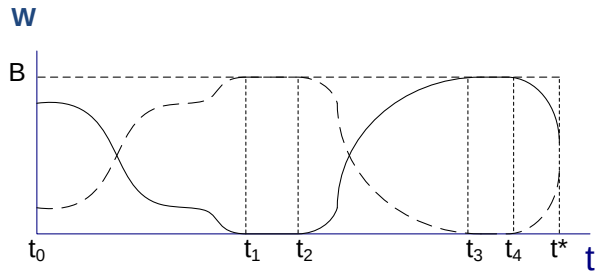

Fig. 9: Workload of the $G/D/1/B/$ and $D/G/1/B$ systems. The dashed line and the solid line represent $\overline{W}(t)$ and $W(t)$ respectively.

[28] J. Vetter, P. Novak, M. Wagner, C. Veit, K. Moller, J. Besenhard, M. Winter, M. Wohlfahrt-Mehrens, C. Vogler, and A. Hammouche, "Ageing mechanisms in lithium-ion batteries," *J. Power Sources*, vol. 147, no. 1-2, pp. 269–281, 2005.

APPENDIX: PROOF OF EQUIVALENCE THEOREM

Let the initial workload state in the storage system, that is, the $D/G/1/B$ system be $W(t_0)$. Then, in the $G/D/1/B/$ model, we set $\overline{W}(t_0) = B - W(t_0)$.

Lemma 1 *If at any time t,* $W(t)+\overline{W}(t) = B$ *then* $W(t^*)+\overline{W}(t^*) = B \ \forall \ t^* > t$.

Proof: Let $t_{2i-1},\ i = 1, 2, \cdots$, be the i^{th} time in the interval $[t \ \ t^*]$ that the storage system becomes either full or empty and persistently in this state until t_{2i} (Figure 9). Similarly, we define $\bar{t}_{2i-1}$ to be the i^{th} time that the buffer in the model becomes either full or empty and persistently in this state until $\bar{t}_{2i}$.

We prove the lemma in two parts. First, we use induction to prove that $t_i = \bar{t}_i$ for all values of i and that if $W(t_{i-1}) + \overline{W}(t_{i-1}) = B$ then $W(t_i) + \overline{W}(t_i) = B$. In the second part, we show that these results hold in the last interval prior to t^*.

Part 1

Base case: Without loss of generality, we assume that $t_1 \leq \bar{t}_1$. Since $W(t)$ and $\overline{W}(t)$ are differentiable on the interval $[t \ \ t_1]$, the Fundamental Theorem of Calculus allows us to write:

$$W(t_1) - W(t) = \int_t^{t_1} dW(s)$$

$$\overline{W}(t_1) - \overline{W}(t) = \int_t^{t_1} d\overline{W}(s)$$

From Section III-A, in this interval we have $dW(t)/dt = -d\overline{W}(t)/dt$. Thus, it can be readily seen that $W(t_1) - W(t) = -(\overline{W}(t_1) - \overline{W}(t))$. Since we have $W(t) + \overline{W}(t) = B$, then $W(t_1) = 0 \ (or \ B)$, implies that $\overline{W}(t_1) = B \ (or \ 0)$, and it implies that $t_1 = \bar{t}_1$.

Inductive step: Given $W(t_k) + \overline{W}(t_k) = B$, we prove that $t_{k+1} = \bar{t}_{k+1}$, and $W(t_{k+1}) + \overline{W}(t_{k+1}) = B$. Again without loss of generality, assume that $t_{k+1} \leq \bar{t}_{k+1}$. Since $W(t)$ and $\overline{W}(t)$ are differentiable on the interval $[t_k \ \ t_{k+1}]$, the Fundamental Theorem of Calculus allows us to write:

$$W(t_{k+1}) - W(t_k) = \int_{t_k}^{t_{k+1}} dW(s)$$

$$\overline{W}(t_{k+1}) - \overline{W}(t_k) = \int_{t_k}^{t_{k+1}} d\overline{W}(s)$$

Since $dW(t)/dt = -d\overline{W}(t)/dt$ in this interval, we have $W(t_{k+1}) - W(t_k) = -(\overline{W}(t_{k+1}) - \overline{W}(t_k))$. Therefore, we conclude that $W(t_{k+1}) + \overline{W}(t_{k+1}) = B$. Clearly, $W(t_{k+1}) = 0 \ (or \ B)$ implies that $\overline{W}(t_{k+1}) = B \ (or \ 0)$, which in turn, results in $t_{k+1} = \bar{t}_{k+1}$.

Part 2

Now assuming that $t_n \leq t^* \leq t_{n+1}$, the last part of the proof is to show that $W(t^*)+\overline{W}(t^*) = B$ given that $W(t_n)+\overline{W}(t_n) = B$. Again, $W(t)$ and $\overline{W}(t)$ are differentiable on the interval $[t_n \ \ t^*]$, and we can write:

$$W(t^*) - W(t) = \int_{t_n}^{t^*} dW(s)$$

$$\overline{W}(t^*) - \overline{W}(t) = \int_{t_n}^{t^*} d\overline{W}(s)$$

Using the fact that $dW(t)/dt = -d\overline{W}(t)/dt$, we can write $W(t^*) - W(t_n) = -(\overline{W}(t^*) - \overline{W}(t_n)$. By induction, we previously showed $W(t_n) + \overline{W}(t_n) = B$; thus, we conclude that $W(t^*) + \overline{W}(t^*) = B$ and the proof is complete. □

Proof of the Equivalence Theorem

It follows from Lemma 1 that there is a one-to-one mapping from trajectories of the $D/G/1/B$ queuing system to trajectories of the $G/D/1/B$ queuing system and that $\forall t, W(t) + \overline{W}(t) = B$. □

Corollary 1 *It follows from the above theorem that:*

$$\mathbb{P}(W(\infty) > B) = \mathbb{P}(\overline{W}(\infty) < 0)$$
$$\mathbb{P}(W(\infty) < 0) = \mathbb{P}(\overline{W}(\infty) > B)$$

Where $W(\infty)$ *is the stationary workload process.*